Theoretical Study of Main-Group Metal−Borazine Sandwich Complexes

Hong Seok Kang†

College of Natural Science, Jeonju University, Hyoja-dong, Wansan-ku, Chonju, Chonbuk 560-759, Republic of Korea

Received: August 18, 2004; In Final Form: November 22, 2004

Using density functional theory within the generalized gradient approximation, we have theoretically studied the formation of neutral metal−aromatic complexes R_1-M and R_1-M-R_2, where M is either neutral lithium, calcium, or gallium and R_1 or R_2 is benzene or borazine. We first find that calcium atom is an effective mediator for cooperative formation of a sandwich complex with borazine, while others are not. When benzene and borazine are mixed in the presence of calcium, a 1:2:1 mixture of benzene−calcium−benzene, borazine−calcium−benzene, and borazine−calcium−borazine is expected. An "A"-shaped structure is predicted for homo- and heterocomplexes of borazine with partial B−B and B−C bonds, while two rings are planar in the case of homocomplexes of benzene. Our analysis of the electron density distributions in HOMO-1 to LUMO in terms of orbital symmetry in conjunction with analysis of *l,m*-projected electronic local density of states shows that this correlates with the charge transfer and the interaction of π^* states of the rings mediated by empty d-states of Ca, which is ultimately related to the polarity of the B−N bond. We find that there is a large accumulation of electron density on particular atoms upon complex formation, predicting characteristic behavior in electron-transfer reaction and nucleophilic reaction different from those for pure benzene or borazine molecule. The hetero-sandwich complex is of particular interest due to its asymmetrical distribution of excess electrons.

1. Introduction

There has been increasing interest in the gas-phase synthesis of organometallic compounds using laser vaporization technique.[1] Motivated by the discovery of $Cr(benzene)_2$,[2] the technique has been extensively applied to metal−benzene complexes, allowing discovery of many kinds of complexes including multiple deckers.[3] Theoretical understanding of their physicochemical properties is also under way.[4] However, most of the works are focused on the transition metal complexes, and there have been only a few works reported for similar complexes of main group elements. Very recently, it has been theoretically shown that Li−aromatic complexes can be also formed.[5] In our previous work, even one-dimensional crystal was proposed for the complex of a large aromatic hydrocarbon, pyrene.[6] Noting that radical anions of aromatic hydrocarbons $R^{\bullet -}$ have been widely used in electron-transfer (ET) reaction[7] and nucleophilic reaction[8] in organic chemistry and it is generated from alkali metal and aromatic hydrocarbon in the form of R−Li, clusters of other main-group elements can be also potentially useful in organometallic chemistry.

Meanwhile, little focus has been given to similar complexes involving borazine, a molecule isoelectronic to benzene. Its aromaticity[9] and complex formation with chromium[10,11] have been of interest in many investigations. According to the author's knowledge, however, a metal−borazine complex involving metals other than chromium remains unexplored. This consideration leads us to investigate sandwich complexes R′−Li−R′, R′−Ca−R′, R−Ca−R, and R′−Ca−R, where R and R′ are benzene and borazine, respectively. Detailed understanding of binding properties, geometrical structures, and electronic structures of these complexes in comparison with those of each other will gives us deeper insight into (1) the difference in the aromaticity of benzene and borazine and (2) the role of empty d-orbitals in such a complex. In addition, it will also find out the possibility of devising a new ET reagent and new classes of organometallic reagents, as well as that of designing new forms of materials. Furthermore, this kind of investigation will allow us to have a better understanding of the interaction of nanotubes with aromatic compounds mediated by such metals, considering that benzene and borazine are the basic building blocks of carbon nanotubes (CNT)[12] and boron nitride nanotubes (BNNT).[13] This will be particularly important for the development of nanoelectronic devices based on BNNT, since it is known to be chemically much less reactive than CNT.

2. Theoretical Methods

Our total energy calculations are performed using the Vienna ab initio simulation program (VASP).[14,15] The electron−ion interaction is described by the projector augmented wave (PAW) method.[16] Wave functions are described in terms of the plane-wave basis, not of localized orbitals. Exchange-correlation effect is treated within the generalized gradient approximation due to Perdew, Burke, and Ernzerhof (PBE).[17] The solution of the Kohn−Sham (KS) equation was obtained using Davison blocked iteration scheme followed by the residual vector minimization method.[15] All the valence electrons of chemical elements were explicitly considered in the KS equation. For calcium, six 3p electrons were also treated as valence electrons, although 3p-(Ca) states lie far below the Fermi level of the system of concern. *k*-space sampling was done with Γ-point. For this, we use supercells with the size $(L_x, L_y, L_z) = (11.0$ Å, 11.5 Å, 16.0 Å), which guarantees the interatomic distance between neighboring cells at least by 8.465 Å except the case when we explicitly consider a crystalline system as will be discussed in

† E-mail: hsk@jj.ac.kr.

10.1021/jp046279d CCC: $30.25
Published on Web 02/02/2005

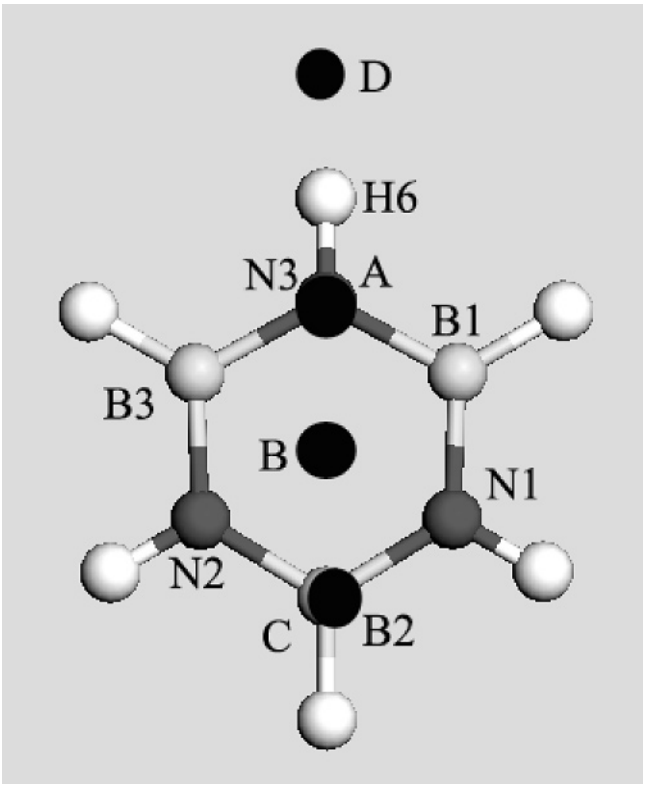

Figure 1. Four possible initial positions (A−D) of a metal atom in its complex with borazine. A−C denote corresponding positions above the borazine ring approximately by 3.9 Å, while position D is located on the plane defined by the ring. Atomic symbols are also defined for borazine to be used in other figures.

the next section. Cutoff energy is set to high (=400 eV) enough to get reliable results, and the conjugate gradient method is employed to optimize the geometry until the Hellmann−Feynman force exerted on an atom is less than 0.03 eV/Å.

3. Results

We first consider the process R′ + Li → R′−Li, where R′ is a borazine molecule. [We also denote benzene by R without prime in the latter part of this section.] For this, we have optimized geometry starting from four different lithium positions. Initial structures A−D represent the lithium atom lying on top of a nitrogen atom, the top of the center of the borazine ring, the top of a boron atom, and 1.5 Å from one of the hydrogen atoms along the direction of a N−H bond, respectively (see Figure 1). When optimized, we find three energy minima. The lowest energy structure "α" has the lithium atom on top of a N−H bond. The distance between the lithium atom and the N−H bond is 2.358 Å. The complex exhibits an overall symmetry of C_s, where the N−H bond gets slightly out of the borazine plane toward the direction opposite to the lithium atom. Structure "β", which has energy marginally higher (=0.02 eV), is characterized by a crystal structure in which the lithium atom bridges two borazine rings belonging to neighboring cells. Namely, there is a linear B−H−Li−H−N connection, where B−H and N−H groups belong to different borazine rings in the neighboring cells. Distances (=3.245 and 3.293 Å) between lithium and hydrogens are nearly the same. The highest energy structure "γ", which is still marginally higher (=0.02 eV) in energy than structure β, also exhibits C_s symmetry, being represented by the lithium atom sitting on top of a boron atom. The interatomic distance between them is 2.872 Å. In all of the conformations, the borazine rings remain planar. The binding

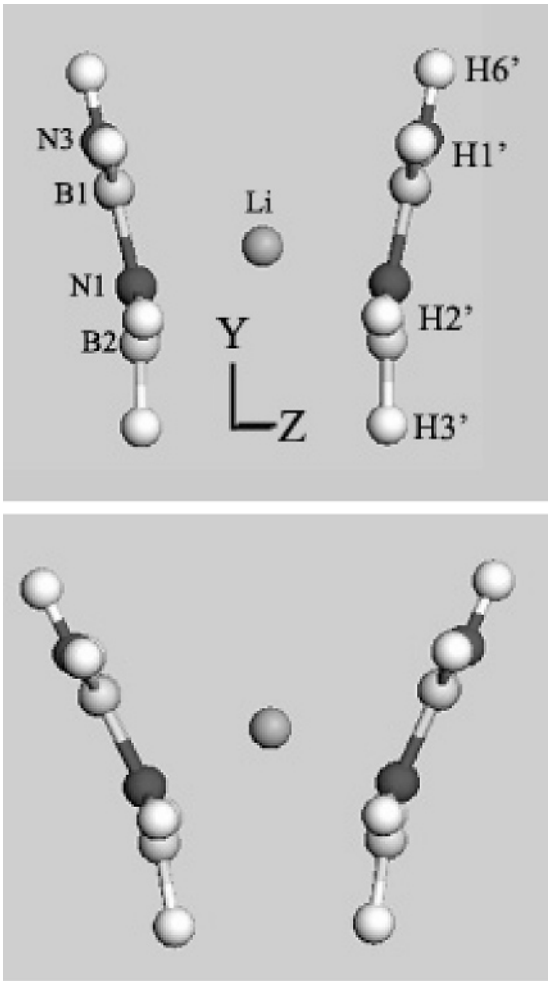

Figure 2. Two optimized conformers a (a) and b (b) of R′−Li−R′ (R′ = borazine) with the same energy. Atomic symbols and the coordinate system are also defined.

energy of structure α is found to be even smaller (=−0.06 eV), which can be compared with our previous result that the benzene−lithium complex exhibits stronger binding with E_b = −0.35 eV.[6] In short, any kind of borazine−lithium complex is not expected to be stable enough to survive the thermal motion.

Next, we consider the sandwich-forming process R′−Li + R′ → R′−Li−R′. For this, we consider two isomers of R′−Li−R′. In the eclipsed isomer *E*, nitrogen atoms of a ring face nitrogen atoms of the other ring when viewed along the direction perpendicular to the ring plane, while those atoms face boron atoms in the staggered isomer *S*. We find that the isomer *E* is more stable than the isomer *S* by 0.31 eV, and our further discussion is focused on this isomer. This observation is in contrast with Bridgeman's prediction[10] on the chromium sandwich complex R′−Cr−R′, which suggested that the staggered isomer is more stable. For this, we want to point out that their calculation is based on an idealized geometry starting from D_{3d} symmetry for the staggered isomer, not on an optimized geometry obtained from full relaxation of geometry for each of isomers *S* and *E* along the direction of ab initio force. In fact, Figure 2 shows that the optimized geometry exhibits much lower symmetry, C_{2v} for isomer *E*. [Our geometry optimization shows that isomer *S* of our Li sandwich complex also exhibit symmetry (=C_{2h}) different from D_{3d}.] There are two different conformations (E_1 and E_2) with the same binding energy (=−0.48 eV). The difference between the two isomers is mainly reflected in the difference in the angle between the two borazine rings. Lithium atom is located approximately on top of hexagons of

TABLE 1: Geometrical Parameters, the Binding Energies (E_b), and the Bond Order between Specified Atoms for Sandwich Complexes R_1-M-R_2, Where M = Lithium or Calcium and R_1 and R_2 Are Either Borazine (R′) or Benzene (R)

		R′−Li−R′				
conformer	R−Li−R[a]	E_1[b]	E_2[c]	R′−Ca−R′	R−Ca−R	R′−Ca−R
l(N3−N3′)[d]	3.746	4.595	5.490	5.205	4.280	5.146
l(B1−B1′)[e]	3.796	4.239	4.781	4.892	4.529	4.688
l(N1−N1′)[f]	3.796	3.627	3.552	3.168	4.529	3.046
l(B2−B2′)[g]	3.746	3.593	3.190	1.925	4.280	1.818
l(M-ring)[h]	1.898	1.967	2.083	2.194	2.265	2.459
θ(ring−ring)[i] (deg)	0	25	50	75	0	75
E_b[j] (eV)	−1.11	−0.54	−0.54	−1.25	−1.39	−1.31
O(B2−B2′)[k]	0.00 (0.00)	0.00 (0.01)	0.00 (0.02)	0.88 (0.83)	0.11 (0.02)	0.76 (0.71)

[a] Results from our previous work in ref 6. [b] Conformer E_1 shown in Figure 2a. [c] Conformer E_2 shown in Figure 2b. [d] N3−N3′ distance for R′−M−R′. For R−Ca−R and R′−Ca−R, it denotes distances between C6−C6′ and N3−C6, respectively. [e] B1−B1′ distance for R′−M−R′. For R−Ca−R and R′−Ca−R, it denotes distances between C1−C1′ and B1−C1, respectively. [f] N1−N1′ distance for R′−M−R′. For R−Ca−R and R′−Ca−R, it denotes distances between C4−C4′ and N1−C4′, respectively. [g] B2−B2′ distance for R′−M−R′. For R−Ca−R and R′-Ca−R, it denotes distances between C2−C2′ and B2−C2, respectively. [h] Approximate distance between the metal atom M and the borazine or benzene ring. [i] Approximate angle between two rings R_1 and R_2. [j] Binding energy for the process $R_1 + R_2 + M \rightarrow R_1-M-R_2$. [k] Bond order of the bond between B2−B2′ or corresponding atoms. The first number corresponds to the Wiberg bond index, while the number in parentheses denote the overlap-weighted natural atomic orbital bond order.

borazine rings. Atoms N3, B1, and N1 lie almost on the same plane, while atom B2 and its equivalent (B2′) slightly repel each other. Table 1 shows geometrical parameters for them. Also shown are the corresponding data for the benzene sandwich complex. Compared to it (D_{2h}) in which two benzene rings are parallel to each other, the borazine complex exhibits much lower symmetry. As a result, N3−N3′ and B1−B1′ distances are longer, while N1−N1′ and B2−B2′ distances are shorter. From now on, a prime on the atomic label denotes that it corresponds to an atom at the equivalent position in the other ring. For example, N3′ is equivalent to N3 under σ_v reflection in Figure 2a. From Table 1, we note that the binding energy (=−0.54 eV) of the overall process $2R' + Li \rightarrow R'-Li-R'$ is about half of that (=−1.11 eV) in the corresponding process for its benzene analogue.[6] In short, the borazine−lithium sandwich complex is less stable than its benzene analogue.

Analysis of the KS energy levels, the *l*,*m*-projected electronic local density of state (LDOS), and the electron density distribution for each of the KS levels will lead us to a clearer picture for this observation. For this, we consider the isomer E_1. There is no significant difference between E_1 and E_2 in their electronic structure. We first find a large (HOMO-1)−HOMO gap (=4.98 eV) originated from the HOMO−LUMO gap (=6.13 eV) of borazine, indicating that all the states up to HOMO-1 are derived from the interactions of molecular states (up to HOMO) of two borazine molecules. Figure 3 shows the electron distribution of this system for HOMO-1, HOMO, and LUMO. HOMO-1 is characterized by (+)HOMO2−(−)HOMO2 interaction, where HOMO2 is one of two degenerate HOMOs of borazine shown in Figure 4a. Different signs in two orbitals denote antibonding interaction between them. Electron density is negligible around lithium. Meanwhile, half-filled HOMO can be represented by (+)LUMO1−p_y(Li)−(+)LUMO1 interaction, where π^* lobes of B1 and N1 overlap the corresponding ones of B1′ (a corresponding atom to B1 in the other ring) and N1′ mediated by one phase of p_y(Li) inside a V-shaped cavity. [See Figure 2a for the definition of the coordinate system.] In addition, the π^* lobe of B2 overlaps that of B2′ through the other phase of p_y(Li). Therefore, an electron in 2s(Li) in the system 2R′ + Li is transferred to this HOMO state upon the formation of the complex R′−Li−R′, and the orbital nature of HOMO described above indicates transfer of almost one electron from Li to borazine rings. LUMO is simply (+)LUMO2−(+)LUMO2 interaction of borazine without contribution from the lithium state. [See Figure 4b,c for the definition of LUMO1 and LUMO2 of borazine.] This also implies that a state derived from the (+)LUMO1−(−)LUMO1 interaction of borazine lies above the LUMO of this sandwich compound. We have also calculated the charge on each atom from the natural bond order analysis[18] (NBO) in the GAUSSIAN03 program[19] using the B3LYP exchange-correlation functional with 6-31G(d) basis. Table 2 indeed shows that there is large charge transfer from lithium to borazine rings comparable to that found in its benzene analogue, evidenced by the charge on the lithium atom, $q(\mathrm{Li}) = +0.879$. As mentioned above, this is consistent with the electron distribution of HOMO delocalized on the borazine rings. When compared with the case of a borazine molecule, Table 2 shows that there is a large decrease in the atomic charge at B2. Much of the charge transferred from the calcium atom is accommodated by B2, which will decrease repulsion between B2 and B2′ and allow them to come closer. This can be also easily understood from the fact that the HOMO of R′−Li−R′ is (+)-LUMO1(R′)−p_y(Li)−(+)LUMO1(R′), if we simply note that the electron density of LUMO1(R′) is largely concentrated on B2, as can be seen from Figure 4b. On one hand, electron density is almost negligible on N3 in LUMO(R′). Evidently, this property of LUMO(R′) is originated from the polarity of the B−N bonds in borazine, which is not observed in benzene. This also suggests that the V-shaped orientation of two borazine rings with respect to each other (θ angle in Table 1) is due to the better interaction among three orbitals, (+)LUMO1(R′), p_y-(Li), and (+)LUMO1(R′) compared to the case of parallel orientation, particularly at sites B2 and B2′. In short, our analysis of the electronic structure of the complex R′−Li−R′, particularly that of HOMO, shows that the formation of the sandwich complex is due to the electrostatic interaction among $(R')^{(-0.5+\delta)}$−$Li^{(+1-2\delta)}$−$(R')^{-(-0.5+\delta)}$, where is δ a small quantity. Geometry of the complex as well as the NBO charges on each atom can be also explained from this analysis.

Now, we are at the stage which allows us to understand the reason the binding energy of the sandwich formation for R′−Li−R′ is small compared to the case of its benzene analogue. We first note that HOMO−LUMO gaps of benzene and borazine are 5.10 and 6.13 eV, respectively. As was noted, the HOMO of R′−Li−R′ is derived from LUMO1 of borazine. Since the LUMO of borazine lies higher than that of benzene with respect to HOMO levels, the energy eigenvalue of the HOMO for R′−Li−R′ cannot get lowered enough by the mere interaction of LUMO1(R′) with the p-state of lithium. In fact, the (HOMO-1)−HOMO gap of this complex is still 4.98 eV,

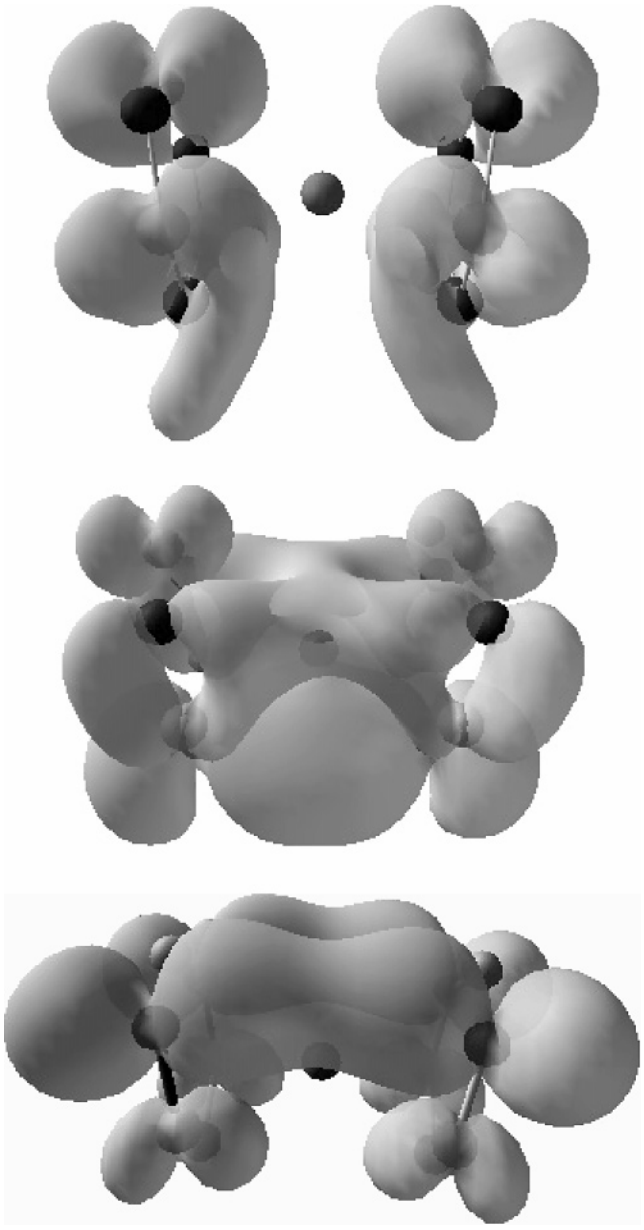

Figure 3. Electron density distributions in HOMO-1 (a), HOMO (b), and LUMO (c) of R′−Li−R′ (R′ = borazine) viewed along *X* axis. For clarity, hydrogen atoms are not shown. See Figure 2 for the definition of the coordinate system.

while the corresponding gap (=4.27 eV) in R−Li−R is 0.71 eV lower even without interacting with a Li-derived state. For this, we note that our separate analysis shows that the HOMO of R−Li−R is represented by the interaction (+)LUMO(R)−(+)LUMO1(R). In short, the HOMO−LUMO gap in borazine, which is much larger than that in benzene, does not allow strong binding upon complex formation after transfer of an electron from the 2s(Li) state to the HOMO of the complex.

A question naturally arises if we can find another neutral metal whose borazine sandwich complex is at least as stable as the benzene−lithium sandwich complex. For this, we consider calcium, since it can make larger charge transfer and its empty d-orbitals can interact with π-states of borazine more efficiently. Therefore, we consider a processes, R′ + Ca → R′−Ca. For this, we have also optimized the geometry of R′−Ca starting from four different positions of the calcium atom depicted in Figure 1. Interestingly, the most stable conformation corresponds to the one-dimensional crystal in which borazine rings are

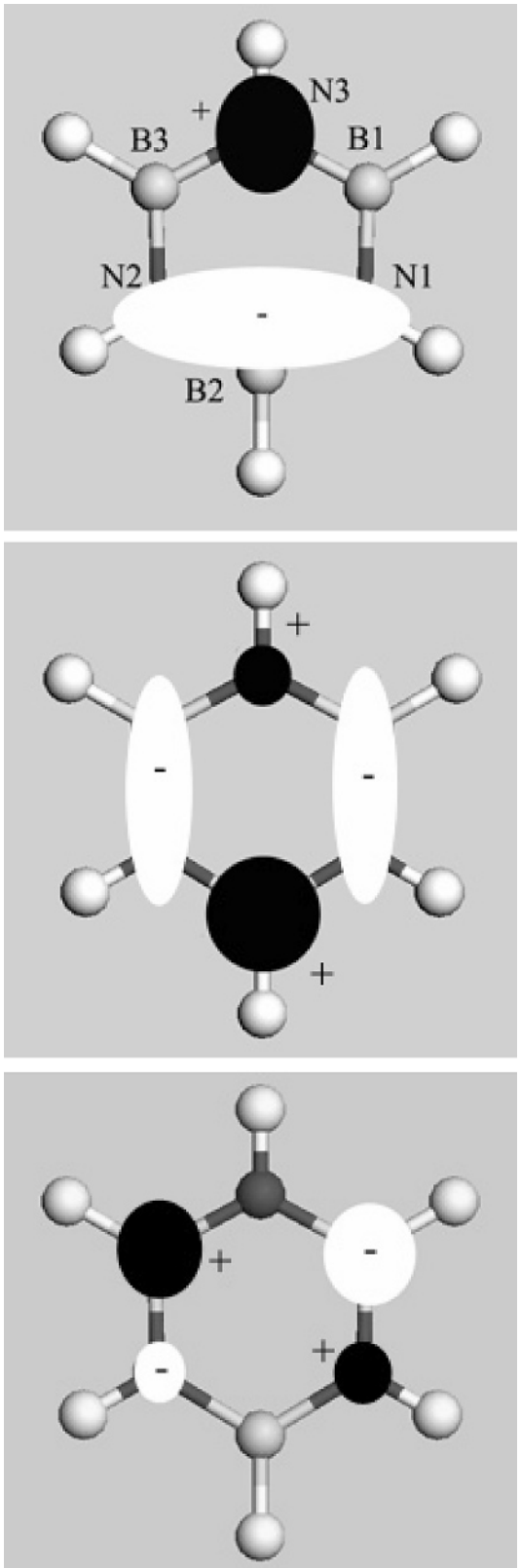

Figure 4. Definition of HOMO2 (a), LUMO1 (b), and LUMO2 (c) of borazine. Black and white elipses denote different phases.

aligned linearly on a plane and there is a linear network of N−H−Ca−H−B between two neighboring cells. This corresponds to structure β for the R−Li complex discussed above. Its binding energy (=−0.05 eV) is even smaller. This observation should correlate with the large HOMO−LUMO gap of borazine. The initial Ca−(H−N) distance was 1.755 Å, and the calcium atom moves away to the interstitial site upon

TABLE 2: Atomic Charges for Various Sandwich Complexes R_1-M-R_2 Calculated from NBO Analysis Based on B3LYP/6-31G(d) Calculations Using the GAUSSIAN03 Program (For Comparison, Also Shown Are Charges for Borazine and Benzene Molecules)

			R′−Li−R′					
	R′	R−Li−R	E_1	E_2	R′−Ca−R′	R	R−Ca−R	R′−Ca−R
q(M)		0.916	0.879	0.785	1.843		1.592	1.819
q(N3)[a]	−1.099	−0.379	−1.119	−1.117	−1.201	−0.238	−0.513	−1.188,[b] −0.665[c]
q(B1)	0.750	−0.294	0.675	0.693	0.633	−0.238	−0.310	0.653, −0.308
q(N1)	−1.099	−0.294	−1.127	−1.132	−1.127	−0.238	−0.310	−1.139, −0.390
q(B2)	0.750	−0.379	0.464	0.484	0.149	−0.238	−0.512	0.452, −0.534
q(H6)[d]	0.427	0.246	0.431	0.430	0.431	0.238	0.251	0.244, 0.433
q(H1)	−0.077	0.245	−0.065	−0.067	0.633	0.238	0.242	0.241, −0.064
q(H2)	0.427	0.245	0.436	0.435	0.428	0.238	0.242	0.233, 0.434
q(H3)	−0.077	0.246	−0.050	−0.046	−0.035	0.238	0.251	0.270, −0.050
q(ring)[e]	0.000	−0.458	−0.440	−0.393	−0.922	0.000	−0.796	−0.583, −1.236

[a] Charge on atom N3 for R′. For R, it denotes C6. Other charges are defined in a similar way. See footnotes in Table 1 for more details. [b] Charge on N3. [c] Charge on C6. [d] Charge on atom H6′ in Figure 2a or on an equivalent position, H6. Other hydrogen atoms are similarly defined. [e] Charge summed for all atoms in R or R′.

optimization. There are three other local minima with energies marginally higher (=0.02 eV) than structure β and almost the same within 0.01 eV among themselves. Two of them correspond to structures α and γ of the R−Li complex, and the last one has the calcium atom on top of the center of the borazine ring.

Now, we consider the overall process $2R' + Ca \rightarrow R'-Ca-R'$. Table 1 shows that its binding energy is more than two times that for R′−Li−R′. In fact, it is even larger than that (=−1.11 eV) for the similar process involving R−Li−R. For this, we have also considered two isomers. Upon optimization, the eclipsed isomer *E* exhibits C_{2v} symmetry, while the staggered isomer *S* shows C_{2h} symmetry. As in the case of its lithium analogue, isomer *S* is found to have weaker binding ($E_b = -0.14$ eV), and further discussion will be focused on isomer *E*. Figure 5 shows its A-shaped optimized structure. At a glance, it is similar to that for its lithium analogue. However, the angle (=75°) between the two borazine rings is much larger, and B2 and B2′ are much closer to each other. (See Table 1.) In addition, borazine rings are folded along the axes joining (B2−N3) and (B2′−N3′). As a result, atom N3 (N3′) protrudes from the plane of the borazine ring toward the calcium atom. On the other hand, atom B2 (B2′) lies almost on the plane. [We have also considered the structure when two borazine rings face each other to form a linear complex of the form ring−N−H−Ca−H−N−ring, finding it to have weak binding ($E_b = -0.04$ eV).]

Investigation of its electronic structure in comparison with that for its lithium analogue will give us better insight into the nature of this structure. In contrast to the case of its lithium analogue discussed above, the (HOMO-1)−HOMO gap (=1.51 eV) is much smaller than the HOMO−LUMO gap (=6.13 eV) of borazine, suggesting a large change of electronic structure upon sandwich formation. Rather, the large (HOMO-2)−LUMO gap (=5.10 eV) suggests that HOMO-2 and LUMO are derived from the HOMO and LUMO of borazine, respectively. This is possible only if a certain kind of level crossing occurs upon sandwich formation. Figure 6 shows electron density distribution for HOMO-1, HOMO, and LUMO. In fact, HOMO-1 is not derived from one of two degenerate HOMOs of borazine. It represents (+)LUMO1(R′)−(−)LUMO1(R′), i.e. antibonding interaction between two LUMO1 states of borazines with negligible electron density around the calcium atom. This is clearly different from the case of R′−Li−R′, for which that antibonding interaction is above LUMO. Although not shown here, HOMO-2 is simply represented by the interaction (+)-HOMO1(R′)−(−)HOMO1(R′), weakly mediated by d_{xz}(Ca), where HOMO1(R′) is the other HOMO of borazine. This implies

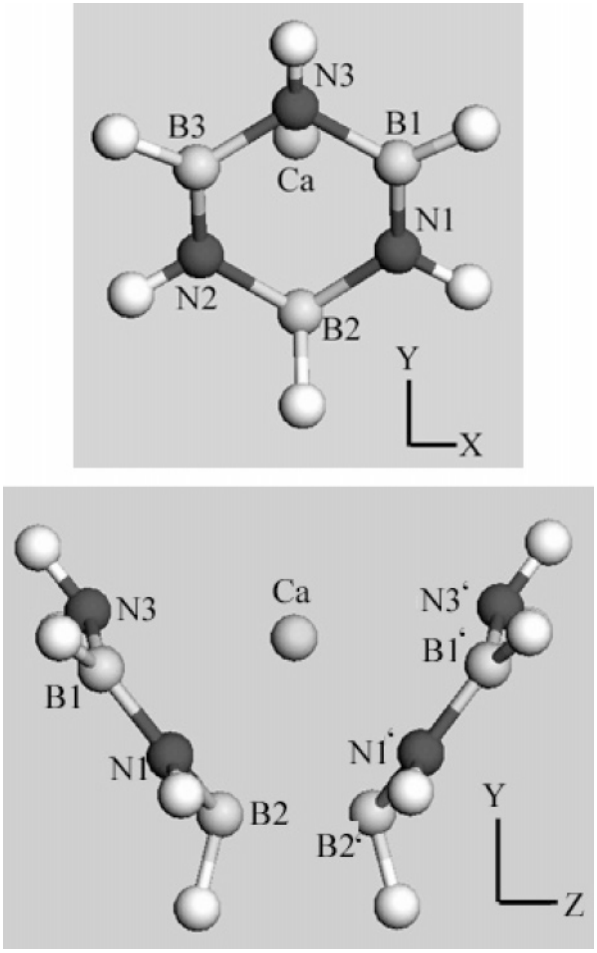

Figure 5. Optimized structure of R′−Ca−R′ (R′ = borazine) projected onto *XY* (a) and *YZ* (b) planes.

that the state (+)HOMO2(R′)−(−)HOMO2(R′) becomes energetically much higher upon complex formation. As will become clear, it lies even above the LUMO of the complex. HOMO, which is fully filled at this time, is characterized by interactions (+)LUMO1(R′)−$3d_{x^2-y^2}$(Ca)−(+)LUMO1(R′), where different phases of $3d_{x^2-y^2}$(Ca) interact with π^* lobes of B2 and N1 according to a simple symmetry consideration of the orbitals. Namely, there are interactions, (+)π^*(B2)−[*y* component of $3d_{x^2-y^2}$(Ca)]−(+)π^*(B2′) and (−)π^*(N1)−[*x* component of $3d_{x^2-y^2}$(Ca)]−(−)π^*(N1′). LUMO is represented by the interaction (+)LUMO2(R′)−$3d_{xy}$(Ca)−(+)LUMO2(R′), where the π^* of B1 (B1′) and B3 (B3′) interact with different phases of $3d_{xy}$-

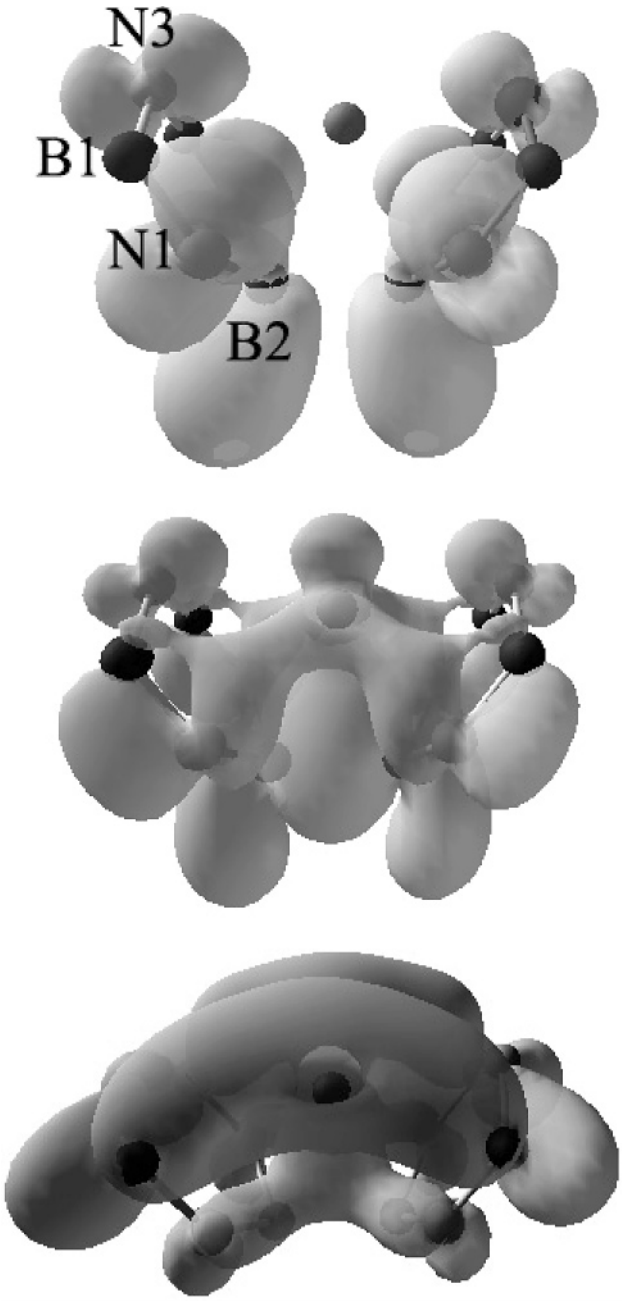

Figure 6. Electron density distributions in HOMO-1 (a), HOMO (b), and LUMO (c) of R′−Ca−R′ (R′ = borazine) viewed along *X* axis. For clarity, hydrogen atoms are not shown. See Figure 5 for the definition of the coordinate system.

(Ca). In summary, HOMO-2, HOMO, and LUMO of the complex are similar to those of R′−Li−R′ in that their orbital natures and the relative phases of the KS orbitals of the borazine molecules involved in each of them are the same beside the participation of 3d(Ca) orbitals instead of 2p(Li) orbitals. Compared to the case of the Li complex, however, the very involvement of 3d(Ca) states is believed to bring about stabilization of filled orbitals around the Fermi level through the formation of A-shaped conformation. In fact, we find that energy eigenvalues of HOMO-1 and HOMO of the complex are lower than those of the corresponding orbitals in R′−Li−R′ by roughly 4 and 2 eV, respectively. This would certainly make an extracontribution to the stabilization of the Ca-sandwich complex with respect to the Li complex even under the severe bending of the B2−H bond. Again, Ca-derived valence states lie above the LUMO of the complex as evidenced by separate analysis of the *l*,*m*-projected LDOS for the Ca atom, indicating transfer of almost two electrons from Ca to the borazine rings. In a sense, we can envision that the sandwich formation is due to the cooperative effect of electrostatic stabilization in $(R')^{(-1+\delta)}$−$Ca^{(+2-2\delta)}$−$(R')^{-(-1+\delta)}$ and the d(Ca)-mediated formation of A-shaped conformation. The NBO charge of calcium (=+1.843) obtained from B3LYP/6-31G(d) calculation is also consistent with this. Positive charge on B2 is even more diminished compared to the case of its lithium analogue, thus allowing closer approach between B2 and B2′ and larger θ angle. In fact, B2 and B2′ gain 0.601 electron per each upon complex formation, the sum of which corresponding to 65% of the total charge transferred from the calcium atom. This can be also expected from the orbital nature of HOMO-1 and HOMO of the complex that have pronounced electron density on B2 and B2′. If HOMO-1 were the interaction (+)HOMO2(R′)−(−)-HOMO2(R′) without level crossing as in the case of the Li complex, we would not expect accumulation of the electron density on B2 which is more pronounced than the case of the Li complex, since HOMO2(R′) exhibits electron density much lower around B2. [See Figure 4.] In short, electrons from the Ca atom are largely transferred to B2 and B2′ of the borazine rings, as clearly manifested in the orbital nature of HOMO-1 and HOMO of the complex, which, in turn, is ultimately related to the polarity of B−N bonds. The B2−B2′ distance (=1.925 Å) corresponds to that for the nonclassical bond in closo-boranes.[20] For this, we have calculated the bond order between these atoms from Wiberg bond index (WBI) analysis and the overlap-weighted natural atomic orbital bond orders (NAO) analysis.[21] Table 1 shows that there is a fractional bond between them, consistent with our finding of the bonding interaction between B2 and B2′ in HOMO. For comparison, we have calculated the bond orders between boron atoms in $P_2B_3H_3$ using the same method, B3LYP/6-31G(d), used for our complex, finding that WBI and NAO orders are 0.46 and 0.49, respectively. These values are in very good agreement with the data (=0.445 and 0.513) for the same bond quoted in Table 2 of ref 20. In brief, the B−B bond in the sandwich complex is stronger than those in closo-boranes. It is also worth noting that each of two borazine rings can hold almost one excess electron, thus forming a radical anion when reacted with calcium metal. (See Table 2.) This sandwich complex might be a reactive intermediate in chemical reactions involving borazine, playing a role similar to that of the lithium−naphthalene complex. When it is subject to a nucleophilic reaction, it is quite possible that the first step is attack of an electrophile to the sandwich complex at B2, not N3, since electron density is richer there in HOMO-1 and HOMO which are close in energy. Hydrogen addition is also expected to occur at B2.

The next question is then how strong the tendency to form R−Ca−R is when R is benzene. For this, we consider the process R + Ca → (R + Ca) (reaction "B1"). The binding energy of R−Ca is still small (=−0.15 eV). In the optimized structure, the benzene ring exhibits a distortion (C_{2v}), adopting a folded conformation. Our analysis of the LDOS shows that the HOMO state is really characterized by one of two degenerate LUMO states of the benzene corresponding to the LUMO1 of borazine shown in Figure 4b. It has the same phase in the wave function on C3 and C6 in Figure 7, interacting with a calcium state derived from the hybridization of 4s and $3d_{x^2-y^2}$ states. The benzene ring is folded along the line joining these atoms so that they are closer (=2.545 Å) to the calcium atom than other carbon atoms in the ring (=2.667 Å). For this, we note that the projection of electron densities around each atom onto

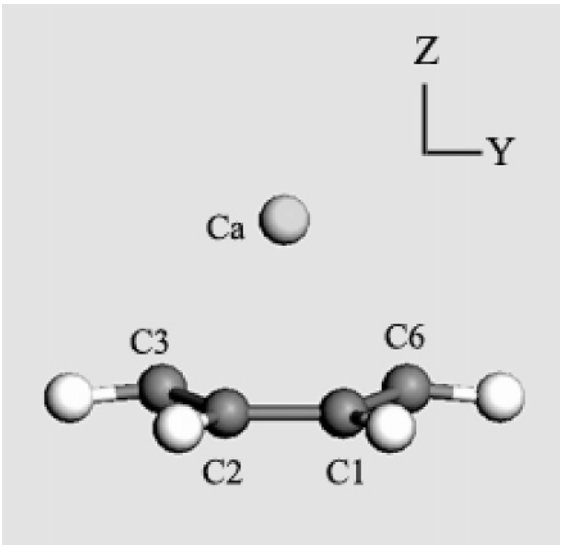

Figure 7. Optimized structure of R−Ca (R = benzene) viewed along *X* axis. The coordinate system is also defined.

each of the angular momentum components shows that atoms C3 and C6 have slightly larger p-character ($sp^{2+\epsilon}$) than other carbon atoms in the ring.

We next consider the process R−Ca + R → R−Ca−R (reaction "B2"). Table 1 shows that the sandwich formation is also cooperative. The binding energy (=−1.39 eV) of the overall process 2R + Ca → (R + Ca + R) is comparable to that for the process 2R′ + Ca → R′−Ca−R′. Meanwhile, this datum also implies that borazine is nearly as effective as benzene in forming a sandwich complex involving calcium, which is contrary to the case of the lithium complex. Figure 8 shows the optimized structure of the sandwich. We first note that two rings are parallel to each other, as can be expected from the nonpolarity of C−C bonds in benzene. Benzene rings are folded, exhibiting D_{2h} symmetry as a whole. The Ca-ring distance (∼2.265 Å) is larger than that (=1.898 Å) for the corresponding Li-sandwich compound by nearly 20%. From the analysis of electron density distribution, we note that HOMO and LUMO of this system have A_g and B_{1g} symmetry, consistent with the fact that they are derived from two degenerate LUMO states (LUMO1, LUMO2) of benzene. [Again, see Figure 4a−c for the definition of the states, HOMO2, LUMO1, and LUMO2, since they are similar to those of borazine.] Figure 9 shows that the electron density distributions for HOMO-1, HOMO, and LUMO are similar to those for R−Li−R and R′−Li−R′ except that d(Ca) states are involved instead of p(Li) states. No level crossing is observed. There is transfer of two electrons from the 4s(Ca) state to the HOMO of the complex, which is practically the LUMO1 of benzene. As was noted before, the HOMO−LUMO gap of benzene, which is smaller than that of borazine, implies that the observed binding energy of the sandwich complex is mainly due to the simple electrostatic interaction in $R^{(-1+\delta)}$−$Ca^{(+2-2\delta)}$−$R^{-(-1+\delta)}$. In fact, HOMO-1 is characterized by interaction (+)HOMO2(R)−p_y(Ca)−(−)-HOMO2(R). HOMO and LUMO are represented by the interactions (+)LUMO1(R)− $3d_{x^2-y^2}$(Ca)−(+)LUMO1(R) and (+)LUMO2(R)−$3d_{xy}$(Ca)−(+)LUMO2(R), respectively. This nature of HOMO and LUMO is manifested in a small (∼0.50 eV) gap between them. Large charge transfer to benzene rings is manifested in our separate NBO analysis based on the B3LYP exchange-correlation functional in the GAUSSIN03 program. We find that q(Ca) = +1.592. A 69% amount of excess electrons is equally distributed on C2, C6, C2′, and C6′, as

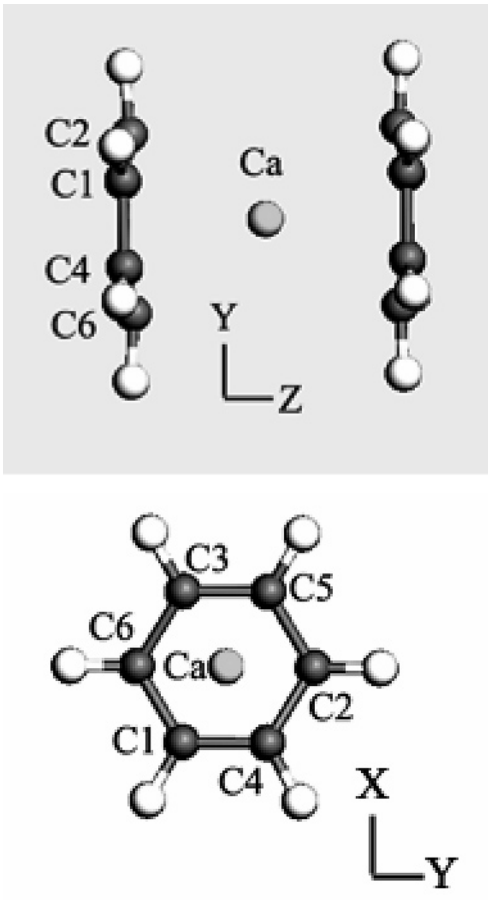

Figure 8. Optimized structure of R−Ca−R (R = benzene) projected onto *YZ* (a) and *XY* (b) planes.

expected from the orbital nature of HOMO again. Therefore, we expect regiospecificity in the nucleophilic reaction, and hydrogen addition of this complex is concentrated on these atoms.

Since we have found that borazine is as effective as benzene in forming a complex of R−Ca−R, it would be also interesting to investigate if the heterocomplex R−Ca−R′ can be formed (R = benzene and R′ = borazine). Interestingly, we observe that the binding energy (=−1.31 eV) of the overall process R + Ca + R′ → R−Ca−R′ is almost the same as those in homocomplexes. On a purely energetic ground, therefore, we can expect that R−Ca−R, R−Ca−R′, and R′−Ca−R′ can be produced approximately in the ratio of 1:2:1 when calcium metal reacts with a mixture of benzene and borazine. Figure 10 shows that its optimized structure is quite similar to that for R′−Ca−R′ (A-shaped) and exhibits C_s symmetry. Benzene ring adopts a folded conformation along C2 and C6. Table 1 shows that the B2−C2′ distance (=1.818 Å) is even smaller than that between B2−B2′ in R′−Ca−R′, also suggesting the formation of a partial bond between them. This is again manifested in its WBI and NAO bond orders (=0.76 and 0.71) shown in Table 1.

Figure 11 shows that HOMO-1 is represented by weak interaction (+)LUMO1(R′)−[hybrid of $3d_{x^2-y^2}$(Ca),$3d_{yz}$(Ca)]−(−)HOMO2(R), where the only appreciable overlap is due to the interaction (+)π*(B2)−[hybrid of $3d_{x^2-y^2}$(Ca),$3d_{yz}$(Ca)]−(+)π*(C2′). π*-orbitals at N1 and N3 do not almost overlap with d-orbitals of calcium. In HOMO-1, the majority of the electron cloud is concentrated on the borazine ring, suggesting that it is derived from LUMO1(R′). We again find the level crossing between states originated from HOMO2(R′) and

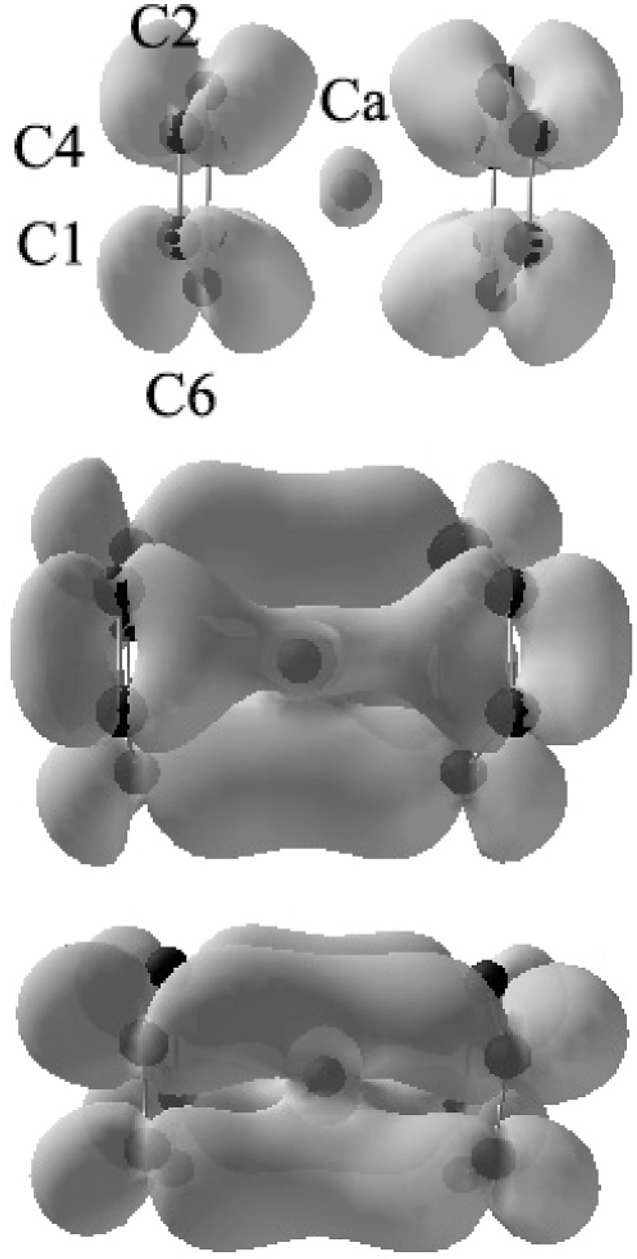

Figure 9. Electron density distributions in HOMO-1 (a), HOMO (b), and LUMO (c) of R−Ca−R (R = benzene) viewed along *X* axis. For clarity, hydrogen atoms are not shown. See Figure 8 for the definition of the coordinate system.

LUMO1(R′) in a way similar to that observed for R′−Ca−R′, piling up electron density around B2. Fully filled HOMO is characterized by even weaker interaction (+)LUMO1(R′)−$3d_{x^2-y^2}$(Ca)−(+)LUMO1(R), implying that it almost corresponds to $3d_{x^2-y^2}$(Ca)−(+)LUMO1(R). Electron density is very small around the borazine ring. In fact, only a small lobe of π*(B2) for LUMO1(R′) takes part in the overlap. LUMO is simply the interaction (+)LUMO2(R′)−$3d_{xy}$(Ca)−(+)LUMO2(R), where π*(B1) and π*(C1) interact one phase of $3d_{xy}$(Ca), while p*(N1) and p*(C4) interact with the other phase. Our separate analysis of the eigenvalues around the Fermi level shows that HOMO-1 and HOMO of the complex are again largely stabilized with respect to those in R′−Li−R′, contributing to the binding of the complex stronger than that for the latter even under the deformations observed in the benzene and borazine rings. In addition, analysis given above shows that there is transfer of two electrons from 4s(Ca) to the HOMO of the

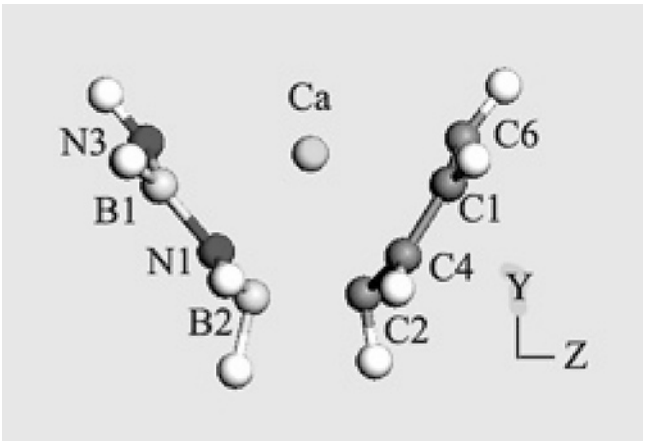

Figure 10. Optimized structure of R′−Ca−R (R′ = borazine; R = benzene) projected onto *YZ* plane.

complex upon complex formation. Furthermore, excess electrons in HOMO transferred from the 4s(Ca) state are mostly accommodated by the benzene ring, as shown in Figure 11b, which is also supported by our NBO charge analysis in Table 2. Namely, q(Ca) = +1.819, q(R) = −1.236, and q(R′) = −0.583, where the latter two are sums of charges for all atoms belonging to each ring. Again, there are large accumulations of excess electron density around B2 in the borazine ring and C6 and C2 of the benzene ring in accordance with our analysis of HOMO-1 and HOMO, among which C6 gets the largest charge (=−0.665). [For this, we can compare charges on each atom in Table 2 with those in benzene and borazine molecules.] In fact, the benzene ring would be extremely reactive due to its ability to hold more than one excess electron. Since it is reasonable to assume that the reaction of this complex with respect to an electrophile or an electron-deficient system is again dominated by the characters of HOMO-1 and HOMO, C2 or C6 of the benzene ring is a possible reaction center.

To elucidate the role of empty d-oribitals in the sandwich complex, we have also considered the process R′ +Ga → R′−Ga (process "Z1"). For this, we find weak binding (E_b = −0.21 eV) on the top of the center of atoms N1, N2, and B2 in Figure 1, where the Ga-ring distance is 2.38 Å. The borazine ring is planar except that B2 and the hydrogen atom attached to it bend from the borazine ring toward the direction opposite to the position of the gallium atom. Other structures are found to be less stable by at least 0.02 eV. The binding energy (=−0.29 eV) of the overall process 2R′ + Ga → R′−Ga−R′ is nearly the same as that for process Z1, implying that there is practically no sandwich formation. Analysis of electronic LDOS and the electron density distribution shows that HOMO-1−LUMO+1 are basically 4s(Ga) and three 4p(Ga) states with only weak interaction with π(R′) states, thus allowing no significant stabilization upon sandwich formation. Similar arguments hold for the corresponding processes involving benzene. In short, we find that filled d-orbitals in Ga do not play any significant role in stabilizing the sandwich complex, which indirectly indicates the crucial role of empty d-orbitals in stabilizing the complex.

4. Conclusions

We have found that neutral calcium atom is an effective mediator for cooperative formation of a sandwich with borazine, while lithium and gallium are not. "A"-shaped structure is expected with borane-type B−B and B−C bond formations between two rings. Interestingly, calcium is also found to form

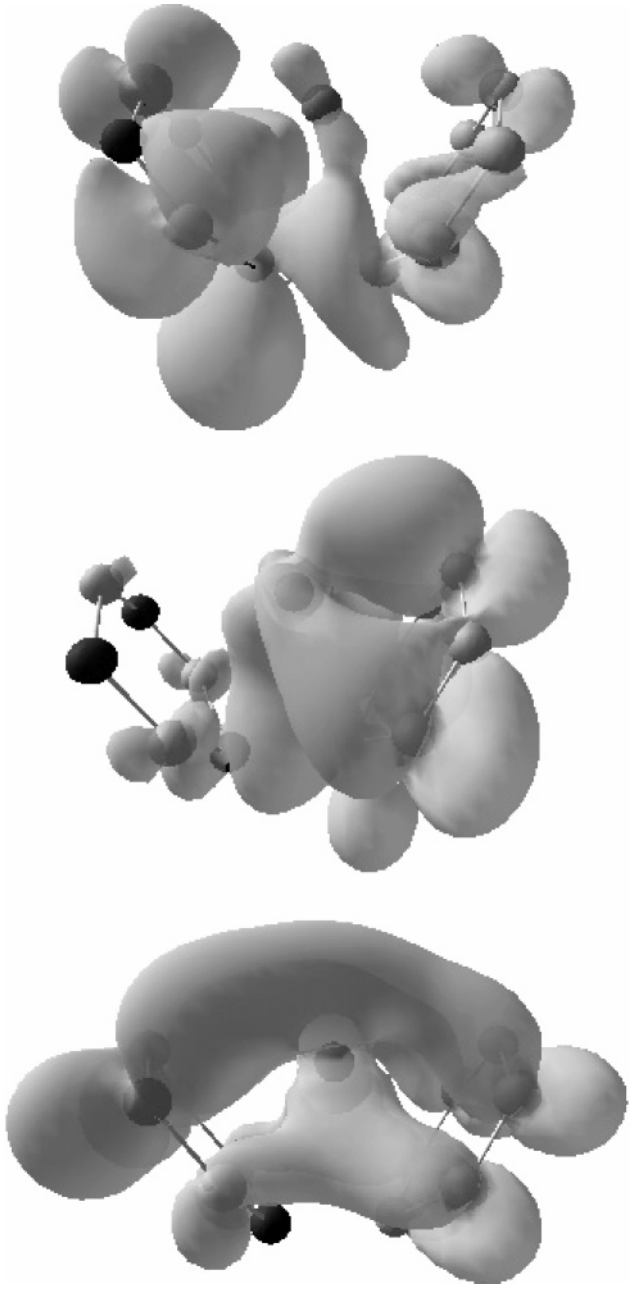

Figure 11. Electron density distributions in HOMO-1 (a), HOMO (b), and LUMO (c) of R′−Ca−R (R′ = borazine; R = benzene) viewed along *X* axis. For clarity, hydrogen atoms are not shown. See Figure 10 for the definition of the coordinate system.

sandwich complexes with benzene with almost the same binding energy. If this comes out to be the case from an experiment, a mixture of benzene and borazine would react with calcium metal, forming complexes benzene−calcium−benzene, benzene−calcium−borazine, and borazine−calcium−borazine approximately in the ratio of 1:2:1. Our analysis of the electron density distribution at each eigenstate around the Fermi level in conjunction with analysis of electronic LDOS shows that this basically correlates with the charge transfer from Ca to borazine or benzene rings upon sandwich formation. Resultant electrostatic interaction is sufficient for the stabilization of benzene−lithium−benzene or benzene−calcium−benzene. However, the HOMO−LUMO gap of borazine, approximately 1 eV larger than that of benzene due to the polarity of B−N bonds, allows only partial stabilization of the complex borazine−lithium−borazine. For this, we note that filled π states of borazine are characterized by enhanced electron density around nitrogen atoms, while unfilled π^* states have electron density richer in boron atoms. Unfavorable electron distribution on electropositive boron atoms in π^* states of borazine brings about a large HOMO−LUMO gap in the molecule. Therefore, simple filling of the LUMO of borazine upon formation of a sandwich complex is energetically less favorable than the case of the benzene complex. Fortunately, we find additional stabilization in the complexes borazine−calcium−borazine and borazine−calcium−benzene originated from the complicated role of empty d(Ca) orbitals coupled with the polar nature of LUMO orbital of borazine. The crucial role of the d(Ca) orbital was elucidated by the electronic structure analysis, being further confirmed by very weak binding in borazine−gallium−borazine complex. Most of the structural and binding properties as well as partial charge distributions can be also explained from this, characters of HOMO-1 and HOMO states playing the most important role.

In the complexes, each of the benzene and borazine rings can accommodate almost one excess electron per ring, forming radial anions, which would act as a very reactive intermediate to be able to transfer electrons to an electron-deficient system or act as a strong nucleophile in various chemical reactions. Again, our analysis of HOMO-1 and HOMO suggests that these reactions would occur in a regiospecific way, which is clearly different from that involving a borazine molecule or a benzene molecule not belonging to such a complex. For example, the previous section suggests that a nucleophile is expected to attack one of the boron atoms at a specific site when the borazine ring is a part of R′−Ca−R′, while the corresponding reaction starts with the attack of an electrophile at nitrogen centers for a borazine molecule in the gas phase.[22] Hetero-sandwich complex benzene−calcium−borazine needs a particular attention, since more than one excess electron is concentrated on the benzene ring, not on the borazine ring. In this system, the polarity of B−N bonds in the borazine ring is propagated to the benzene ring through empty d-orbitals of calcium, which may have an implication in information technology based on molecular devices.

For more practical applications to organic or inorganic reactions, it may be desirable to extended calculations to the complexes of larger aromatic systems, such as naphthalene, pyrene, and their borazine analogues, since they would accommodate excess electrons more easily.

Acknowledgment. We thank Jeonju University for financial support.

References and Notes

(1) (a) Teh, C. S.; Willey, K. F.; Robbins, D. L.; Pilgrim, J. S.; Duncan, M. A. *Chem. Phys. Lett.* **1992**, *196*, 233. (b) Higashide, H.; Kaya, T.; Kobayashi, M.; Shinohara, H.; Sato, H. *Chem. Phys. Lett.* **1990**, *171*, 297. (c) Holland, P. M.; Castleman, A. W., Jr. *J. Chem. Phys.* **1982**, *76*, 4195. (d) Robels, E. S. J.; Ellis, A. M.; Miller, T. A. *J. Chem. Phys.* **1992**, *96*, 8791. (e) Misaizu, F.; Sanekata, M.; Fuke, K.; Iwata, S. *J. Chem. Phys.* **1994**, *100*, 1161. (f) Mitchell, S. A.; Blits, M. A.; Siegbahn, P. E.; Svensson, M. *J. Chem. Phys.* **1994**, *100*, 423.

(2) Fischer, E. O.; Hafner, W. Z. *Naturforsch.* **1955**, *10B*, 665.

(3) (a) Nakajima, A.; Kaya, K. *J. Phys. Chem. A* **2000**, *104*, 176. (b) Kurikawa, T.; Takeda, A.; Hirano, M. Judai, K.; Arita, T.; Nagano, S.; Nakajima, A.; Kaya, K. *Organometallics* **1999**, *18*, 1430. (c) Clock, F. G. N.; Dix, A. N.; Green, J. C.; Perutz, R. N.; Seddon, E. A. *Organometallics* **1983**, *2*, 1150. (d) Andrews, M. P.; Mattar, S. M.; Ozin, Z. A. *J. Phys. Chem.* **1986**, *90*, 1037.

(4) (a) Pandey, R.; Rao, B. K.; Jena, P.; Blanco, M. A. *J. Am. Chem. Soc.* **2001**, *123*, 3799. (b) Sahnoun, R.; Mijoule, C. *J. Phys. Chem. A* **2001**, *105*, 6176. (c) Bauschlicher, C. W., Jr.; Partridge, H.; Langhoff, S. R. *J. Phys. Chem.* **1992**, *96*, 3273.

(5) Vollmer, J. M.; Kandalam, A. K.; Curtiss, L. A. *J. Phys. Chem. A* **2002**, *106*, 9533.
(6) Kang, H. S. *J. Phys. Chem. A* **2005**, *109*, 478.
(7) (a) Holy, N. L. *Chem. Rev.* **1974**, *74*, 245. (b) Yus, M.; Herrera, R. P.; Guijarro, A. *Chem. Eur. J.* **2002**, *8*, 2574.
(8) Herrera, R. P.; Guijarro, A.; Yus, M. *Tetrahedron Lett.* **2003**, *44*, 1313.
(9) (a) Steiner, E.; Fowler, P. W.; Havenith, R. W. A. *J. Phys. Chem. A* **2002**, *106*, 7048. (b) Kiran, B.; Phukan, A. K.; Jemmis, E. D. *Inorg. Chem.* **2001**, *40*, 3615. (c) Fink, W. H.; Richards, J. C. *J. Am. Chem. Soc.* **1991**, *113*, 3393. (d) Matsunaga, N.; Gordon, M. S. *J. Am. Chem. Soc.* **1994**, *116*, 11407. (e) Jemmis, E. D.; Kiran, B. *Inorg. Chem.* **1998**, *37*, 2110.
(10) Bridgeman, A. J. *Polyhedron* **1998**, *17*, 2279.
(11) (a) Huttner, G.; Krieg, B. *Angew. Chem., Int. Ed. Engl.* **1971**, *10*, 512. (b) Huttner, G.; Krieg, B. *Chem. Ber.* **1972**, *105*, 3437. (c) Lagowski, J. J. *Coord. Chem. Rev.* **1977**, *22*, 185. (d) Brown, D. A.; McCormack, C. G.; *Chem. Commun. (London)* **1967**, 383.
(12) *Science and Application of Nanotubes*; Tomanek, D., Enbody, R. J., Eds.; Kulwer Academic: New York, 2000.
(13) (a) Rubio, A.; Corkill, J. L.; Cohen, M. L. *Phys. Rev. B* **1994**, *49*, 5081. (b) Chopra, N. G.; Luyken, R. J.; Cherrey, K.; Crespi, V. H.; Cohen, M. L.; Louie, S. G.; Zettl, A. *Science* **1995**, *269*, 966.
(14) Kresse, G.; Hafner, J. *Phys. Rev. B* **1993**, *47*, RC558.
(15) Kresse, G.; Furthmuller, J. *Phys. Rev. B* **1996**, *54*, 11169.
(16) Kresse, G.; Joubert, D. *Phys. Rev. B* **1999**, *59*, 1758.
(17) Perdew, J. P.; Burke, K.; Ernzerhof, M. *Phys. Rev. Lett.* **1996**, *77*, 3865.
(18) Reed, A. E.; Curtiss, L. E.; Weinhold, F. *Chem. Rev.* **1988**, *88*, 899.
(19) Frisch, M. J.; Trucks, G. W.; Schlegel, H. B.; Scuseria, G. E.; Robb, M. A.; Cheeseman, J. R.; Montgomery, J. A., Jr.; Vreven, T.; Kudin, K. N.; Burant, J. C.; Millam, J. M.; Iyengar, S. S.; Tomasi, J.; Barone, V.; Mennucci, B.; Cossi, M.; Scalmani, G.; Rega, N.; Petersson, G. A.; Nakatsuji, H.; Hada, M.; Ehara, M.; Toyota, K.; Fukuda, R.; Hasegawa, J.; Ishida, M.; Nakajima, T.; Honda, Y.; Kitao, O.; Nakai, H.; Klene, M.; Li, X.; Knox, J. E.; Hratchian, H. P.; Cross, J. B.; Adamo, C.; Jaramillo, J.; Gomperts, R.; Stratmann, R. E.; Yazyev, O.; Austin, A. J.; Cammi, R.; Pomelli, C.; Ochterski, J. W.; Ayala, P. Y.; Morokuma, K.; Voth, G. A.; Salvador, P.; Dannenberg, J. J.; Zakrzewski, V. G.; Dapprich, S.; Daniels, A. D.; Strain, M. C.; Farkas, O.; Malick, D. K.; Rabuck, A. D.; Raghavachari, K.; Foresman, J. B.; Ortiz, J. V.; Cui, Q.; Baboul, A. G.; Clifford, S.; Cioslowski, J.; Stefanov, B. B.; Liu, G.; Liashenko, A.; Piskorz, P.; Komaromi, I.; Martin, R. L.; Fox, D. J.; Keith, T.; Al-Laham, M. A.; Peng, C. Y.; Nanayakkara, A.; Challacombe, M.; Gill, P. M. W.; Johnson, B.; Chen, W.; Wong, M. W.; Gonzalez, C.; Pople, J. A. *Gaussian03*, Revision B.05; Gaussian, Inc.: Pittsburgh, PA, 2003.
(20) Schleyer, P. v. R.; Subramanian, G.; Dransfeld, A. *J. Am. Chem. Soc.* **1996**, *118*, 9988.
(21) (a) Reed, A. E.; Weinstock, R. B.; Weinhold, F. *J. Chem. Phys.* **1985**, *83*, 735. (b) Reed. A. E.; Weinhold, F. *Chem. Rev.* **1988**, *88*, 899. (c) Reed, A. E.; Schleyer, P. v. R. *J. Am. Chem. Soc.* **1990**, *112*, 1434.
(22) (a) Chiavarino, B.; Crestoni, M. E.; Fornarini, S. *J. Am. Chem. Soc.* **1999**, *121*, 2619. (b) Chiavarino, B.; Crestoni, M. E.; Marzino, A. D.; Fornarini, S.; Rosi, M. *J. Am. Chem. Soc.* **1999**, *121*, 11204.